http://dx.doi.org/10.11142/jicems.2013.2.4.466

Novel DC Grid Connection Topology and Control Strategy for DFIG-based Wind Power Generation System

Xilu Yi *, and Heng Nian **

Abstract – The paper presents a novel DC grid connection topology and control strategy for doubly-fed induction generator (DFIG) based wind power generation system. In order to achieve the wind power conversion, the stator side converter and the rotor side converter is used to implement the DFIG control based on the indirect air-gap flux orientation, and a DC/DC converter is used for the DFIG system to DC grid connection. The maximum power point tracking and DC voltage droop control can also be implemented for the proposed DFIG system. Finally, a 4-terminal DFIG-based multi-terminal DC grid system is developed by Matlab to validate the availability of the proposed system and control strategy.

Keywords: Doubly-fed induction generator, Indirect air-gap flux orientation, Maximum power point tracking, DC voltage droop control, Multi-terminal DC grid system

1. Introduction

With the development of large-scale and off-shore wind power generation, the grid connection technology for the wind farms becomes more and more essential [1]. Voltage source converter (VSC) based multi-terminal high voltage direct current (MTDC) transmission system is considered as an attractive option for grid connection of off-shore wind power generation, instead of using the classical AC transmission method. The wind farms and AC grids can be connected by VSC-MTDC to implement the wind power transmission and integration, which is beneficial to power quality, grid stability and the flexibility of transmission system [2-6].

Up to now，the wind power generation systems based on DFIG has been used most widely, due to the significant characteristics such as flexible regulation of active and reactive power and lower requirement for converter capacity. In [7], the traditional MTDC topology for DFIG-based wind farm was used, in which DFIG is connected to the DC bus using a wind farm side VSC followed by a 3ph AC transformer. This system configuration is complicated and power generation performance will be deteriorated due to the weak grid in the wind farm. In [8], a novel topology using DC-DC converter to step up the DC voltage to HVDC level for power transmission is mentioned. The line frequency transformer is replaced by high power DC-DC converter with medium frequency, which brings the significant reduction in overall size and weight.

In this paper, a new DFIG-based MTDC system with simpler DC grid connection topology and control method is proposed, as shown in Fig. 1. A stator side converter (SSC) with a DC-DC converter and a rotor side converter (RSC) fed by DC bus is connected to DFIG. The isolated DC-DC converter is used to step up the DC voltage to HVDC system. Unlike the traditional MTDC system, the proposed DFIG based HVDC system has simpler structure and higher stability due to the elimination of wind farm side VSCs and 3ph transformers. It also should be pointed out that the DC voltage of HVDC connection point can be regulated by SSC and DC/DC converter, which is beneficial for the DC voltage management of HVDC system.

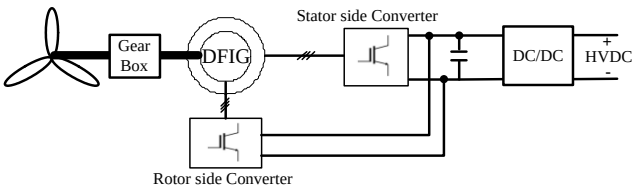

Fig. 1. The proposed DFIG system unit for HVDC connection

In order to implement the DC bus voltage management of HVDC connection point for DFIG system, DFIG should be controlled as a voltage source instead of a current source. In [9] and [10], the indirect stator flux orientation (ISFO)

* Dept. of Electrical Engineering, Zhejiang University, China. (yxl00655@gmail.com)
** Dept. of Electrical Engineering, Zhejiang University, China. (nianheng@zju.edu.cn)
Received 13 October 2013; Accepted 31 October 2013

control method was discussed to implement the stator voltage control DFIG. The sensorless control based on ISFO was presented in [11] with the rotor speed estimation by an adaptive observer. However, the proposed methods mainly aimed at stand-alone DFIG system and the voltage control, which is not suitable for the proposed system for HVDC connection. In [12], ISFO control was applied in HVDC system based on line commutated converters, in which the classical frequency and voltage droop characteristics were used to achieve the control of active and reactive power.

An important issue in MTDC is the stable operation capability of DC grid, which can be implemented by coordinating the control of multiple grid side VSCs (GSVSC) and wind farm side VSCs (WFVSC) [13]. In the traditional MTDC system for wind farm, only GSVSC participates in DC grid management, WFVSCs are controlled as current source for the energy conversion. When the VSC for DC management disconnects from DC grid or loses control due to grid fault, or when wind farms employ larger ratio in the grid power, the power of MTDC system will be unbalanced [14]. It should be pointed out that DFIG system should participate in the DC grid management and stabilize the DC voltage by regulating the power captured from the wind turbine.

In this paper, a novel DC grid connection topology and control strategy for DFIG-based wind power generation system was proposed. The modified indirect air-gap flux orientation control method is proposed and implemented by RSC, and the SSC is controlled to regulate the power transmitted from DFIG to DC grid. And then, a DC voltage droop control is used in SSC to achieve the DC voltage management of MTDC system. Finally, the effectiveness of the proposed system and control strategy is validated by the MATLAB simulation based on a 4 terminal DFIG-based MTDC system.

2. Modeling and Control Strategy of DFIG

The proposed DFIG system for HVDC connection is shown in Fig.1. The SSC is directly connected to the stator of DFIG and controlled as a rectifier to regulate the wind power from DFIG to DC grid. The RSC is responsible to achieve the control of the air-gap electromotive force (EMF) of DFIG.

Due to the direct connection between the SSC and DFIG, the traditional vector control method based on stator voltage or flux orientation is not suitable for the proposed system. The modified indirect air-gap flux orientation control method for RSC and the air-gap EMF orientation control method for SSC are proposed in this paper.

2.1 Rotor Side Converter

Unlike the AC grid-connected condition, the air-gap flux and EMF of DFIG will not be determined by the stator voltage, which will be regulated by the rotor magnetizing current.

In the air-gap flux orientation control method, the air-gap flux angle θ_m can be derived based on the frequency reference of the air-gap EMF. By aligning the *d*-axis on the air-gap flux vector of DFIG, the flux and EMF equations of DFIG can be written as following on the synchronous rotating d-q reference frame,

$$\begin{cases} \psi_{dm} = L_m i_{ds} + L_m i_{dr} = L_m i_m \\ \psi_{qm} = L_m i_{qs} + L_m i_{qr} = 0 \\ \psi_{ds} = L_s i_{ds} + L_m i_{dr} \\ \psi_{qs} = L_s i_{qs} + L_m i_{qr} \\ \psi_{dr} = L_r i_{dr} + L_m i_{ds} \\ \psi_{qr} = L_r i_{qr} + L_m i_{qs} \\ e_{dm} = \dfrac{d\psi_{dm}}{dt} - \omega_1 \psi_{qm} \\ e_{qm} = \dfrac{d\psi_{qm}}{dt} + \omega_1 \psi_{dm} \end{cases} \tag{1}$$

where, i_{ds}, i_{qs}, i_{dr}, i_{qr} represent the stator current and rotor current in d-q axis respectively; Ψ_{dm} and Ψ_{qm} represent the d and q axis component of the air-gap flux respectively; Ψ_{ds} and Ψ_{qs} represent the d and q axis component of the stator flux respectively; Ψ_{dr} and Ψ_{qr} represent the d and q axis component of the rotor flux respectively; e_{dm} and e_{qm} are the d and q axis component of the air-gar EMF respectively; ω_1 is the angular velocity of the air-gap EMF; L_m is the magnetic inductance; L_s is the stator inductance of DFIG; L_r is the rotor winding inductance; i_m is the magnetizing current.

The magnetizing current reference can be written as,

$$i_m^* = \frac{|E_m^*|}{\omega_1 L_m} \tag{2}$$

where, E_m^* is the amplitude reference of the air-gap EMF.

Based on (1), the rotor current *q*-axis reference i_{qr}^* can be presented as,

$$i_{qr}^* = -i_{qs} \tag{3}$$

The rotor voltage equations of DFIG can be written as,

$$\begin{cases} u_{dr} = R_r i_{dr} + \dfrac{d\psi_{dr}}{dt} - (\omega_1 - \omega_r)\psi_{qr} \\ u_{qr} = R_r i_{qr} + \dfrac{d\psi_{qr}}{dt} + (\omega_1 - \omega_r)\psi_{dr} \end{cases} \tag{4}$$

where, R_r is the rotor resistance and ω_r is the rotor speed.

Therefore, the reference of rotor voltage component in *d-q* axis can be written as,

$$\begin{cases} u_{dr}^* = (k_{pr} + k_{ir}/s)(i_{dr}^* - i_{dr}) - \omega_s L_{\sigma r} i_{qr} \\ u_{qr}^* = (k_{pr} + k_{ir}/s)(i_{qr}^* - i_{qr}) + \omega_s L_{\sigma r} i_{dr} + \omega_s L_m i_m \end{cases} \tag{5}$$

where, $L_{\sigma r} = L_r - L_m$; ω_s=ω_1-ω_r; k_{pr} and k_{ir} are the proportional and integral coefficient of the PI regulator for rotor current respectively.

The *d* axis component of the stator voltage can be written as,

$$u_{ds} = R_s i_{ds} + \frac{d\psi_{ds}}{dt} - \omega_1 \psi_{qs} \tag{6}$$

According to (1) and (3), (6) can be rewritten as,

$$i_m + \frac{L_m}{R_s}\frac{di_m}{dt} = i_{dr} + \frac{1}{R_s} e_{dm} \tag{7}$$

Considering that e_{dm} is equal to zero on the steady state according to (1), thus, the *d* axis component of rotor current i_{dr}^* can be controlled by the PI regulator on the error of magnetizing current.

The vector control scheme of RSC in DFIG system is shown in Fig. 2. The error of magnetizing current Δi_m is sent into the PI regulator to output i_{dr}^*. And the rotor current i_{dr} and i_{qr} are controlled via two independent PI regulators. Finally, SVPWM is used to implement the RSC control.

2.2 Stator Side Converter

Considering that the stable air-gap EMF can be implemented by RSC, the SSC can adopt the air-gap EMF orientation control strategy to implement the DFIG power output.

To implement the air-gap EMF orientation, the air-gap EMF vector angle θ_v can be presented as,

$$\theta_v = \theta_m + \pi/2 \tag{8}$$

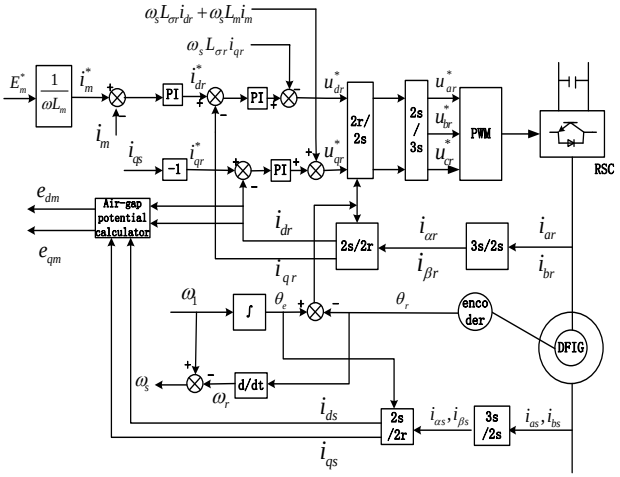

Fig. 2. The control scheme of RSC

The stator flux and voltage equations of DFIG can be written as,

$$\begin{cases} \psi_{ds} = L_s i_{ds} + L_m i_{dr} \\ \psi_{qs} = L_s i_{qs} + L_m i_{qr} \\ u_{ds} = i_{ds} R_s + L_{\sigma s}\dfrac{di_{ds}}{dt} + e_{dm} - \omega_1 L_{\sigma s} i_{qs} \\ u_{qs} = i_{qs} R_s + L_{\sigma s}\dfrac{di_{qs}}{dt} + e_{qm} + \omega_1 L_{\sigma s} i_{ds} \end{cases} \tag{9}$$

where, u_{ds} and u_{qs} are the d and q axis component of the stator voltage respectively; $L_{\sigma s} = L_s - L_m$.

The reference of stator voltage component in d-q axis can be written as,

$$\begin{cases} u_{ds}^* = (k_{ps} + k_{is}/s)(i_{ds}^* - i_{ds}) + e_{dm} - \omega_1 L_{\sigma s} i_{qs} \\ u_{qs}^* = (k_{ps} + k_{is}/s)(i_{qs}^* - i_{qs}) + e_{qm} + \omega_1 L_{\sigma s} i_{ds} \end{cases} \tag{10}$$

The control diagram of SSC is shown in Fig. 3. Based on

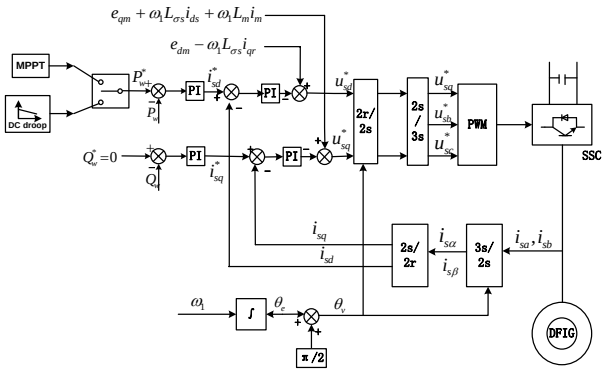

Fig. 3. The control scheme of SSC

the air-gap EMF orientation, the current component i_{ds} is proportional to the stator active power while the current component i_{qs} determines the reactive power.

In the proposed control strategy, the reactive power reference is set as zero to guarantee unity power factor operation of SSC. The active power reference can be achieved either by the maximum power point tracking (MPPT) control or DC voltage droop control, depending on the DC management condition, which will be illustrated in section III.

3. Power Control of SSC

In MTDC system, it is important to implement the DC grid stabilization by coordinating the control of multiple grid side VSCs (GSVSC) and wind farm side VSCs (WFVSC). In the proposed DFIG-based MTDC system, the SSC for DFIG grid connection can operate as a GSVSC to participate in the transmission power control in the HVDC bus, as the SSC can regulate the stator active power output. Usually, DFIG can operate on MPPT mode and output all the power captured by the wind turbine. When the HVDC system needs DFIG to take the responsibility of DC grid management, the proposed DFIG-based MTDC system can be operated on the DC voltage droop mode to participate in the DC voltage control among VSCs.

3.1MPPT Control

In order to achieve maximum energy generation under the variable wind speed conditions, the reference of the active power in SSC control scheme is set according to the MPPT curve of the DFIG. Therefore, the DFIG can realize MPPT operation when the active power reference is set with the cube of the DFIG's rotor speed.

3.2 DC Voltage Droop Control

The DC voltage-current droop control is widely studied in the MTDC transmission system to coordinate the DC voltage stabilization among GSVSCs. The droop control approach eliminates the communication requirement for the converters in the overall HVDC system, which provides higher stability and coordinating DC voltage control capability. To implement the DC voltage control in the DC grid connection point of DFIG system, a modified DC voltage-power droop characteristic is adopted in the wind farm side SSC, as shown in Fig. 4 (a). It can be seen that the power output reference of the DFIG droops linearly along with the increase of the DC voltage. The parameter of the droop curve is determined by the DC grid characteristic for the DFIG connection, for instance, larger gradient of curve brings faster dynamic response but deteriorate stability [13].

To realize the smooth transition between the droop control and the MPPT control of the SSC, a cluster of paralleled droop curves is presented as shown in Fig. 4 (b), in which V_{dc0} is determined by the maximum power and the curvilinear gradient. Each curve corresponds to the MPPT operation under certain wind speed. When the operation mode of the SSC changes from MPPT to droop control, the system will select the right droop curve according to the MPPT power reference.

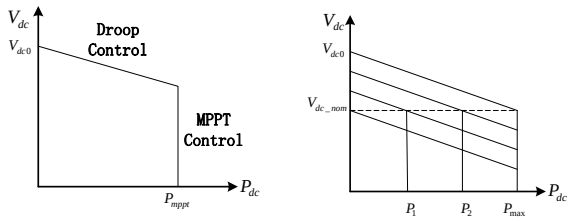

(a) (b)

Fig. 4. DC voltage-power droop characteristic. (a) Droop characteristic of SSC. (b) Droop characteristics considering MPPT operation.

It should be noted that, in the droop control mode, the power transmitted by the SSC may not be equal to that captured by the wind turbine and the rest power will be stored in the mechanic inertia of DFIG, which will lead to the acceleration of the rotor.

4. Simulation Analysis

The operation performance of the proposed DFIG based HVDC system was investigated by developing the 4-terminal MTDC simulation system using MATLAB /Simulink, as show in Fig. 5. The system consists of two 3MW DFIG-based wind turbines and two GSVSC stations. The DC grid system topology and control strategy can be extended to wind farms with multiple DFIGs. The ratings and parameter values of the DFIG is shown in Table 1.

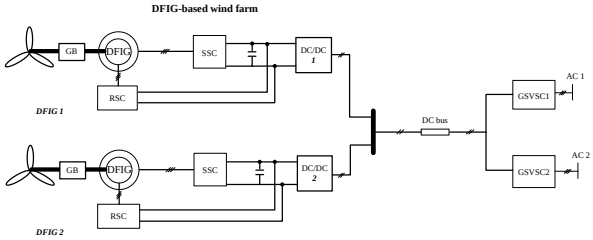

Fig. 5. The 4-terminal HVDC system structure

Table 1. Ratings and Parameters of the DFIG

Data	Code	Parameter
Rated voltage	V_{nom}	690 V
Rated power	P_{nom}	3 MW
Rated speed	n_{nom}	1000 rpm
Rated frequency	F_{nom}	50 Hz
Number of pole pairs	p	3
Sampling frequency	f_s	6 kHz
SVPWM frequency	f_{PWM}	3 kHz

Additionally, the GSVSCs connected to the HVDC grid can operate in DC voltage droop mode or work as a constant voltage regulator, according to the requirement in different operation condition. In this paper, GSVSC1 will operate as the constant DC voltage regulator with the upper limit of power $P_{1(max)}$ set as 1pu. The GSVSC2 will work in the DC voltage droop mode, in which the active power $P_{2(initial)}$ is set as 0.2pu during the rated DC voltage and the upper limit $P_{2(max)}$ is set as 1pu. The voltage-power characteristics of GSVSC1 and GSVSC2 are shown in Fig. 6. In the DC-DC converter, a full bridge circuit creates a high-frequency square wave at the primary side of the transformer, which steps up the voltage to a higher level. A diode bridge at the secondary side of the transformer rectifies the high voltage square wave to the HVDC bus [15].

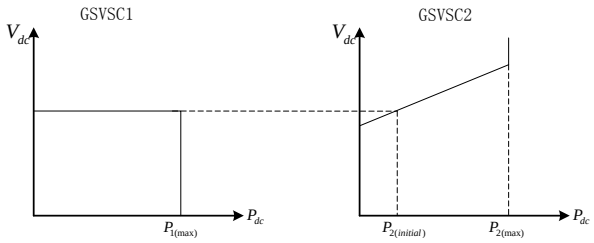

Fig. 6. Droop characteristic of GSVSC1 and GSVSC2

The rated DC voltage of the HVDC system is 10kV. A capacitor bank of 850μF is paralleled at the DC side of each converter. To investigate the effect of actual DC cables on the operation, a resistance R=1.5Ω and inductance L=0.005H is connected in series with the DC cable. The droop characteristic for DFIG1 and DFIG2 is set as $V_{dc}=V_{dcg0}-k_gP_{dc}$, where k_g=1kV/MW and V_{dcg0}=8kV. The droop characteristic for DFIG1 and DFIG2 is set as $V_{dc}=V_{dcw0}-k_wP_{dc}$, where k_w=1kV/MW and V_{dcw0} is decided by the MPPT condition.

The steady-state performance of the proposed control strategy is presented in Fig. 7, in which the active power reference is set as 1 pu while the reactive power reference is 0pu. The rotor speed keeps at 0.8pu during the steady state. Fig. 7 (a) shows the sinusoidal air-gap EMF of DFIG1, and the stator current and the rotor current are shown in Fig. 7 (b)~(c), in which the THD of the stator and rotor current is 1.02% and 1.13% respectively. It can be seen that DFIG can have the stable operation performance on the air-gap flux orientation control strategy.

Fig. 8 shows the MPPT operation results of DFIG with the wind speed in wind farm 1stepping from 8m/s to 12m/s at 0.6s. The maximum power outputs of DFIG1 changes from 0.25pu to 0.73pu during the wind speed variation.

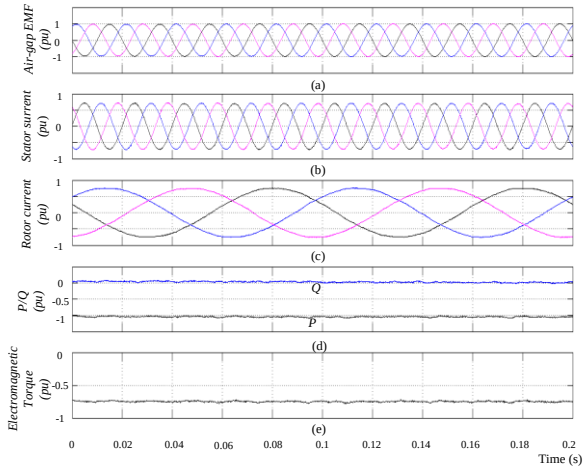

Fig. 7. DFIG operation performance under the proposed control strategy. (a) Air-gap EMF. (b) Stator current. (c) Rotor current. (d) Active power and reactive power output by SSC. (e) Electromagnetic torque.

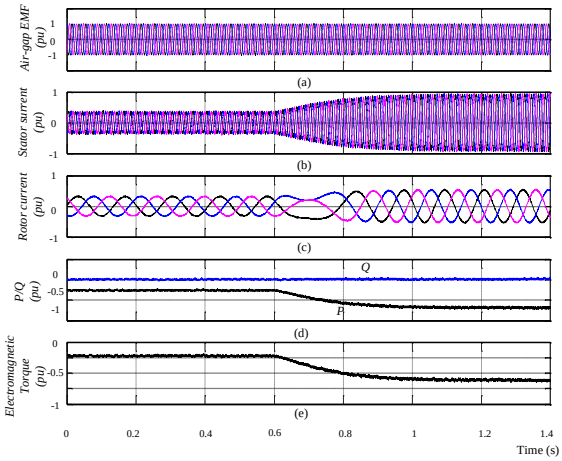

Fig. 8. MPPT performance under wind speed variation. (a) Air-gap EMF. (b) Stator current. (c) Rotor current. (d) Active power and reactive power output by SSC. (e) Electromagnetic torque

Fig. 9 shows the operation performance of the HVDC system with the wind speed in wind farm 1stepping from 8m/s to 12m/s at 0.2s. The wind speed in wind farm 2 is set as 8m/s. The wind power injected to the DC grid will be absorbed by AC grid1, which will lead to the power

increase through GSVSC1 due to the wind speed change. Since the power flowing through GSVSC1 is less than the upper limit 1pu even when wind speed in wind farm 1 is 12m/s, the droop mode of DFIGs and GSVSC2 is disabled and the power in GSVSC2 is kept at 0.2pu. GSVSC1 acts as the DC voltage regulator and keeps the DC voltage in the HVDC bus at 10kV.

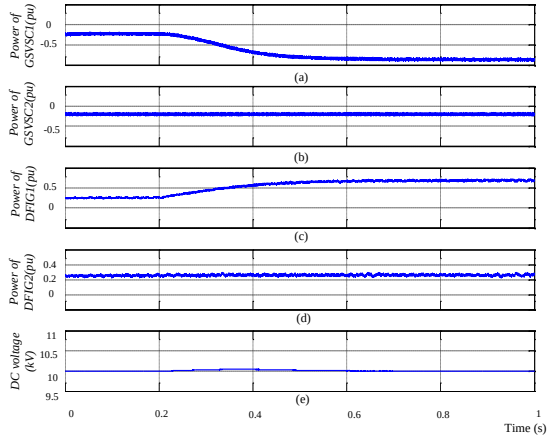

Fig. 9. Simulation results when the wind speed steps from 8m/s to 12ms. (a) Active power output by GSVSC1. (b) Active power output by GSVSC2. (c) Active power output by DFIG1. (d) Active power output by DFIG2. (e) DC voltage of HVDC

Fig. 10 shows the voltage-power droop control results of the DFIG with the wind speed in wind farm 1stepping from 8m/to 14m/s at 0.2s. It can be seen that the power and rotor speed of DFIG1 increases during 0.2s~0.4s to track the MPPT point. The power flowing in GSVSC1 reaches its limit at 0.6s, which will activate the voltage-power droop mode of GSVSC2 and the DFIGs. Considering that the droop characteristic of the DFIG is chosen according to the wind speed, the V_{dc0} in Fig. 4 is set as 2.2pu for DFIG1 and 0.65pu for DFIG2. Consequently, power in GSVSC2 is slightly higher than 0.2pu and power of the DFIGs is just slightly lower than their maximum power, due to the droop control characteristic. The power transferred through GSVSC1 is kept at 1pu and the DC voltage is kept at 10.3kV as shown in Fig. 10 (e). Since the steady state during the droop control period is closed to the MPPT condition, the rotor speed of the DFIGs almost keeps the same.

Fig. 11 shows the operation results when GSVSC1 disconnects from HVDC system, in which the wind speed is set as 12m/s in wind farm 1 and 8m/s in wind farm 2. It can be seen that, when GSVSC1 works in the HVDC system, the power and rotor speed of DFIG1 and DFIG2 increases during 0s~0.3 s to search the MPPT point with the maximum power outputs are 0.73pu from DFIG1 and

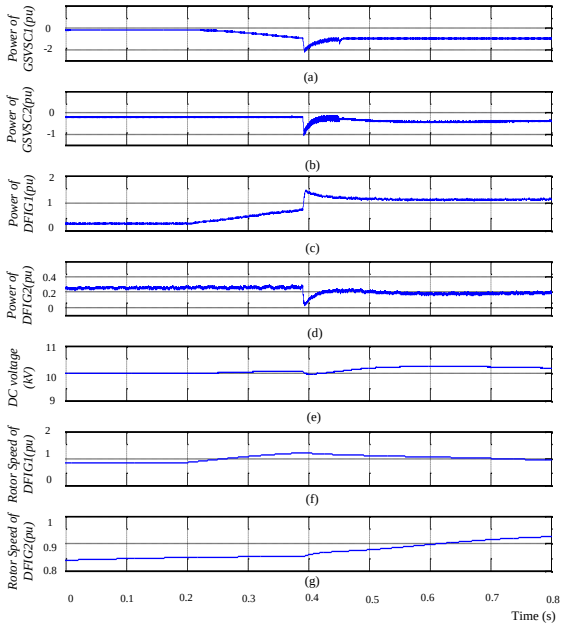

Fig. 10. Simulation results when the wind speed steps from 8m/s to 14ms. (a) Active power output by GSVSC1. (b) Active power output by GSVSC2. (c) Active power output by DFIG1. (d) Active power output by DFIG2. (e) DC voltage of HVDC. (f) Rotor speed of DFIG1. (g) Rotor speed of DFIG2.

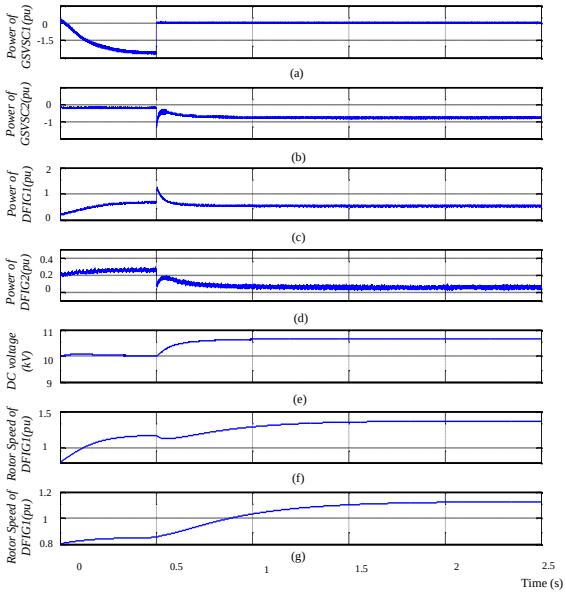

Fig. 11. Simulation results when GSVSC1 disconnects from the DC grid. (a) Active power output by GSVSC1. (b) Active power output by GSVSC2. (c) Active power output by DFIG1. (d) Active power output by DFIG2. (e) DC voltage of HVDC. (f) Rotor speed of DFIG1. (g) Rotor speed of DFIG2.

0.25pu from DFIG2. GSVSC1 is suddenly disconnected from the DC grid at 0.5s. Under this condition, the voltage-

power droop mode of GSVSC2 and DFIGs will be enabled. With the coordinating of SSC of DFIG and GSVSC2, the power transmitted through GSVSC2 increases while power through the two SSCs decreases correspondingly. The DC voltage is therefore limited and stabilized at 10.8kV. The rotor of DFIGs accelerates for the unequal of the power transferred by the SSC and that captured by the wind turbine, as shown in Fig. 11 (f) and (g).

5. Conclusion

A novel DC grid connection topology for DFIG-based wind farm with DC voltage droop control method is proposed in this paper, in which the DFIG is controlled by an indirect flux orientation strategy. The control strategy for DFIG can guarantee the steady voltage output and power regulation ability according to the control requirement. Simulation results validate availability of the control strategy for the proposed DFIG system with the operation in the MTDC system.

Acknowledgements

This work was supported by the National Natural Science Foundation of China under Project 51277159.

References

[1] Luke Livermore, Jun Liang, and Janaka Ekanayake, "MTDC VSC technology and its applications for wind power" in *Proc. of Universities Power Engineering Conference* (*UPEC*), Cardiff, Wales, 2010, pp. 1-6.

[2] P.Bresesti, W. L. Kling, R. L. Hendriks, and R. Vailati, "HVDC connection of offshore wind farms to the transmission system", *IEEE Transactions on Energy Conversion*, vol. 22, no. 1, pp. 37-43, March 2007.

[3] Jun Liang, Tianjun Jin, and Oriol Gomis-Bellmunt, "Operation and control of multi-terminal HVDC transmissions for offshore wind farms", *IEEE Transactions on Power Delivery*, vol. 26, no. 4, pp. 2596-2604, Oct. 2011.

[4] Lie Xu, Barry Wayne Williams, Liangzhong, and Z. Yao, "Multi-terminal DC transmission system for connection large offshore wind farms" in *Proc. Power and Energy Society General Meeting*, Pittsburgh, PA. 2008, pp. 1-7,

[5] T. Nakajima, and S. Irokawa, "A control system for HVDC transmission by voltage sourced converters" in *Proc. IEEE Power Eng. Soc. Summer Meeting*, Edmonton, Alta, 1999, pp. 1113-1119.

[6] Muyeen S M, Rion T, and Junji T. "Operation and control of HVDC-connected offshore wind farm," *IEEE Transactions on Sustainable Energy*, vol. 1, no. 1, pp. 30-37, April 2010.

[7] Xingjia Yao, Hongxia Sui, and Zuoxia Xing, "The study of VSC-HVDC transmission system for offshore wind power farm," in *Proc. of International Conference on Electrical Machines* (*ICEMS*), Seoul, Korea, 2007, pp.314-319.

[8] Wu Chen, Alex Huang, and Srdjan Lukic, "A comparison of medium voltage high power DC/DC converters with high step-Up conversion ratio for offshore wind energy systems," in *Proc. of Energy Conversion Congress and Exposition* (*ECCE*), Phoenix, AZ, 2011, pp.584-589.

[9] Pena R., Clare J.C., and Asher G.M., "A doubly fed induction generator using back-to-back PWM converters supplying an isolated load from a variable speed wind tuibine," *IEEE Proceedings on Electrical Power Applications*, vol. 143, no.5, pp. 380-387, September 1996.

[10] D. Forchetti, G. Garcia and M. I. Valla, "Vector control strategy for a doubly-fed stand-alone induction generator" in Proc. of Industrial Electronics Conference (IECON),2002, vol. 2, pp. 991-995, Sevilla, Spain.

[11] R. Cardenas, R. Peiia, J. Proboste, G. Asher, and J. Clare, "Sensorless control of a doubly- ped induction generator for stand alone operations," in *Proc. of Power Electronics Specialists Conference* (*PESC*), 2004, pp. 3378-3383.

[12] M. Fazeli, S.V. Bozhko, G.M. Asher, and L.Yao, "Voltage and frequency control ororrshore DFIG-based wind farms with line commutated HVDC connection," in *Proc. of IET Conference on Power Electronics, Machines and Drives* (*PEMD*), York, 2008, pp. 335-339.

[13] Shu Zhou, Jun Liang, Oriol Gomis-Bellmunt, Janaka Ekanayake, and Nicholas Jenkins, "Control of multi-terminal VSC-HVDC transmission system for off-shore wind power generation " in *Proc. of Universities Power Engineering Conference* (*UPEC*) , Glasgow, 2009, pp. 1-5.

[14] T. Sakurai and K. Goto, "A new control method for multiterminal HVDC transmission without fast communication systems," *IEEE Transaction on Power Apparatus and Systems*, vol.102, no.5, pp.1140-1150, May 1983.

[15] S. M. Muyeen, R. Takahashi, T. Murata, and J. Tamura, "Control strategy for HVDC interconnected DC-based offshore wind farm", in *Proc. of International Conference on Electrical Machines and Systems* (*ICEMS*), Tokyo, 2009, vol. 1, pp.1-6.

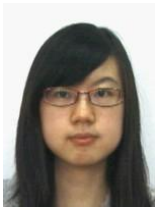

Xilu Yi received the B.Eng. degree and is now pursuing her master degree in electrical engineering from Zhejiang University. His research interests are the DC grid connection technology for DFIG based wind power generation system.

Heng Nian received the B.Eng. degree and the M.Eng. degree from HeFei University of Technology, China, and the Ph.D. degree from Zhejiang University, China, in 1999, 2002, and 2005 respectively, all in electrical engineering. From 2005 to 2007, he was as a Post-Doctoral with the College of Electrical Engineering, Zhejiang University, China. Since 2007, he has been employed as an associate professor at the College of Electrical Engineering, Zhejiang University, China. His current research interests are the optimal design and operation control for wind power generation system.